CHIN. PHYS. LETT. Vol. 37, No. 10 (2020) 107503

Magnetic Phase Diagram of $Cu_{4-x}Zn_x(OH)_6FBr$ Studied by Neutron-Diffraction and μSR Techniques

Yuan Wei(魏源)[1,2†], Xiaoyan Ma(马肖燕)[1,2†], Zili Feng(冯子力)[1,3], Devashibhai Adroja[4,5], Adrian Hillier[4], Pabitra Biswas[4], Anatoliy Senyshyn[6], Andreas Hoser[7], Jia-Wei Mei(梅佳伟)[8], Zi Yang Meng(孟子杨)[1,9,10], Huiqian Luo(罗会仟)[1,10*], Youguo Shi(石友国)[1,10*], and Shiliang Li(李世亮)[1,2,10*]

[1]*Beijing National Laboratory for Condensed Matter Physics, Institute of Physics, Chinese Academy of Sciences, Beijing 100190, China*
[2]*School of Physical Sciences, University of Chinese Academy of Sciences, Beijing 100190, China*
[3]*Institute for Solid State Physics, University of Tokyo, Kashiwa 277-8581, Japan*
[4]*ISIS Facility, Rutherford Appleton Laboratory, Chilton, Didcot Oxon OX11 0QX, United Kingdom*
[5]*Highly Correlated Matter Research Group, Physics Department, University of Johannesburg, PO Box 524, Auckland Park 2006, South Africa*
[6]*Heinz Maier-Leibnitz Zentrum (MLZ), Technische Universität München, Garching D-85747, Germany*
[7]*Helmholtz-Zentrum Berlin für Materialien und Energie, D-14109 Berlin, Germany*
[8]*Shenzhen Institute for Quantum Science and Engineering, and Department of Physics, Southern University of Science and Technology, Shenzhen 518055, China*
[9]*Department of Physics and HKU-UCAS Joint Institute of Theoretical and Computational Physics, The University of Hong Kong, Pokfulam Road, Hong Kong, China*
[10]*Songshan Lake Materials Laboratory, Dongguan 523808, China*

(Received 23 July 2020; accepted 27 August 2020; published online 29 September 2020)

We systematically investigate the magnetic properties of $Cu_{4-x}Zn_x(OH)_6FBr$ using the neutron diffraction and muon spin rotation and relaxation (μSR) techniques. Neutron-diffraction measurements suggest that the long-range magnetic order and the orthorhombic nuclear structure in the $x = 0$ sample can persist up to $x = 0.23$ and 0.43, respectively. The temperature dependence of the zero-field μSR spectra provides two characteristic temperatures, T_{A_0} and T_λ, which are associated with the initial drop close to zero time and the long-time exponential decay of the muon relaxation, respectively. Comparison between T_{A_0} and T_M from previously reported magnetic-susceptibility measurements suggest that the former comes from the short-range interlayer-spin clusters that persist up to $x = 0.82$. On the other hand, the doping level where T_λ becomes zero is about 0.66, which is much higher than threshold of the long-range order, i.e., ∼0.4. Our results suggest that the change in the nuclear structure may alter the spin dynamics of the kagome layers and a gapped quantum-spin-liquid state may exist above $x = 0.66$ with the perfect kagome planes.

PACS: 75.50.Mm, 75.30.Kz, 76.75.+i DOI: 10.1088/0256-307X/37/10/107503

The two-dimensional (2D) kagome antiferromagnetic (AFM) system has attracted a great deal of interest since strong geometrical frustration effects can give rise to various ground states.[1−7] Especially, it has been suggested to be one of the best platforms to realize quantum spin liquids (QSLs), which are highly entangled quantum magnetism that typically, though not necessarily, shows no long-range magnetic order down to zero K.[8,9] Up to date, the most studied kagome $S = 1/2$ magnetic material is the herbertsmithite, $ZnCu_3(OH)_6Cl_2$, which is believed to host a QSL ground state.[10−13] However, there is no consensus on whether its low energy excitations are gapped or gapless,[14−19] which is crucial for us to understand the nature of the QSL state. One of the major difficulties lies in the fact that there is always a few percent of Cu^{2+} ions sitting on Zn^{2+} sites, which mainly affect the low-energy spin excitations.[17,20]

Recently, there are new materials that also consist of 2D Cu^{2+} kagome layers.[21−27] While most of them have magnetic orders, the Zn-doped barlowite [$Cu_3Zn(OH)_6FBr$] provides a promising new platform to study the QSL physics. The structure of barlowite $Cu_4(OH)_6FBr$ is composed of 2D Cu^{2+} kagome

Supported by the National Key Research and Development Program of China (Grant Nos. 2017YFA0302900, 2016YFA0300500, 2018YFA0704200, 2017YFA0303100, and 2016YFA0300600), the National Natural Science Foundation of China (Grant Nos. 11874401, 11674406, 11674372, 11961160699, 11774399, 12061130200, 11974392, and 11822411), the Strategic Priority Research Program(B) of the Chinese Academy of Sciences (Grant Nos. XDB25000000, XDB07020000, XDB33000000, and XDB28000000), the Beijing Natural Science Foundation (Grant Nos. Z180008 and JQ19002), Guangdong Introducing Innovative and Entrepreneurial Teams (Grant No. 2017ZT07C062), the Youth Innovation Promotion Association of CAS (Grant No. 2016004), and the Royal Society-Newton Advanced Fellowship (Grant No. NAF\R1\201248).
†Yuan Wei and Xiaoyan Ma contributed equally to this work.
*Corresponding authors. Email: hqluo@iphy.ac.cn; ygshi@iphy.ac.cn; slli@iphy.ac.cn
© 2020 Chinese Physical Society and IOP Publishing Ltd

layers with Cu^{2+} ions in between and shows long-range AFM order at 15 K.[28–30] Substituting interlayer Cu^{2+} with Zn^{2+} can completely destroy the order and one expects a QSL ground state when no interlayer Cu^{2+} exists.[29,31,32] Indeed, the system shows no magnetic ordering down to 50 mK although its dominant AFM exchange interaction is about 200 K.[23] More interestingly, both NMR and inelastic neutron scattering results suggest that it has a gapped QSL ground state.[23,33] Compared to the herbertsmithite, it has higher crystal symmetry, which gives rise to smaller Dzyaloshinskii–Moriya interaction (DMI)[34,35] and thus makes it further away from the quantum phase transition resulted from the DMI interaction.[36] Moreover, symmetry lowering of the lattice has been observed in the herbertsmithite but not in $Cu_3Zn(OH)_6FBr$.[37–40]

While the Zn-doped barlowite shows its advantages in studying QSL physics on a 2D kagome lattice, it still suffers the same magnetic-impurity issues as the herbertsmithite.[23,33] To further address the role of interlayer Cu^{2+} spins, we have systematically studied the $Cu_{4-x}Zn_x(OH)_6FBr$ system via neutron-diffraction and muon-spin-relaxation (μSR) techniques. The long-range magnetic order and low-temperature orthorhombic structure are observed in the neutron-diffraction experiments for x up to 0.23 and 0.43, respectively. The zero-field (ZF) μSR spectra can be fitted by a phenomenological function, which gives two parameters A_0 and λ, corresponding to the extrapolated zero-time asymmetry and long-time relaxation rate, respectively. We provide a phase diagram of the $Cu_{4-x}Zn_x(OH)_6FBr$ system by combining previous bulk and μSR results.[29,32] Our results are consistent with a gapped ground state in $Cu_3Zn(OH)_6FBr$.

Polycrystalline $Cu_{4-x}Zn_x(OH)_6FBr$ samples were synthesized by the hydrothermal method reported previously.[29] The content of Zn is determined by the inductively coupled plasma (ICP) method. The neutron-diffraction data were obtained on SPODI at FRM-Ⅱ, Germany, WOMBAT at ANSTO, Australia, and the instrument E9 at HZB, Germany. The nuclear and magnetic structures are refined using the FULLPROF program.[41] The μSR experiments were carried out in the longitudinal field (LF) geometry in ZF using the MuSR and EMU spectrometers of the ISIS facility at the STFC Rutherford Appleton Laboratory, Oxfordshire, U.K. The samples were mounted on a 99.995% silver plate, applying dilute GE varnish covered with a high-purity silver foil. The μSR data were analyzed by the Mantid software.[42]

Figure 1(a) shows the neutron powder diffraction intensities for the $x = 0.3$ and 0.69 samples at 20 K. It has been shown that the low-temperature nuclear structure of the $x = 0$ sample is orthorhombic with the space group of $Pnma$.[29] To see whether the orthorhombic structure exists in these two samples, we show the data at high Q, which shows several orthorhombic peaks for the $x = 0.3$ sample but none for the $x = 0.69$ sample. Refinements of the data demonstrate that the lattice space group of the $x = 0.3$ sample is $Pnma$, the same as that for the $x = 0$ sample.[29] The structure of the $x = 0.69$ sample is hexagonal with the space group of $P6_3/mmc$ as that of the $x = 0.92$ sample.[23] Figure 1(b) gives the $(1,0,2)_O$ peak for different samples, which shows that the orthorhombic structure may still present in the $x = 0.43$ sample. Future studies are needed to determine at which doping level the orthorhombic structure disappears.

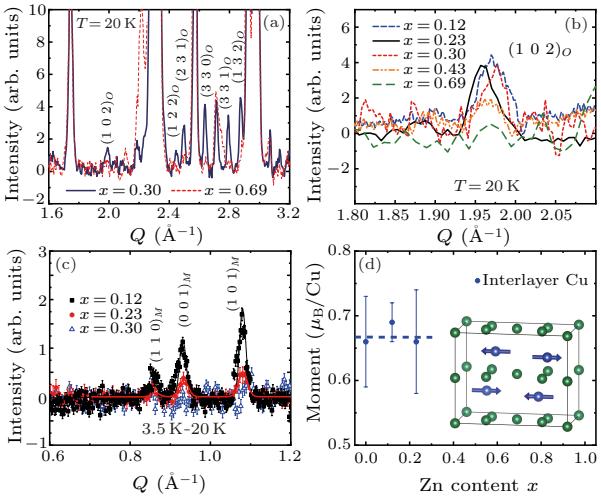

Fig. 1. (a) Neutron powder diffraction intensities for $x = 0.3$ and 0.69 samples at 20 K in the range of large Q's. The labeled peaks correspond to the orthorhombic peaks in the $Pnma$ space group. (b) The $(1,0,2)_O$ peaks for x from 0.12 to 0.69 samples at 20 K. (c) First three magnetic peaks for the $x = 0.12$, 0.23 and 0.3 samples obtained by subtracting the 20-K data from the 3.5-K data. The solid lines show the calculated results for the magnetic structure as reported in Ref. [29]. All the data in (a), (b) and (c) have been normalized by major nuclear peaks after background subtraction. It should be pointed out that since different instruments have different resolutions, the normalization only provides a rough guide. (d) Zn content dependence of the magnetic moment for the interlayer Cu^{2+} ions. The inset presents the crystal and magnetic structures of the $x = 0$ sample, showing only Cu^{2+} ions with the solid lines representing the orthorhombic unit cell. The arrows on the interlayer Cu^{2+} ions indicate the directions of the magnetic moments. Note that some of the Cu^{2+} ions in the top and bottom kagome planes are in the outside of the unit cell.[29]

Figure 1(c) shows the first three magnetic peaks for the $x = 0.12$ and 0.23 samples, which can be refined by the same magnetic structure as in barlowite.[29] In this structure as shown in the inset of Fig. 1(d), the ordered moment mainly comes from the interlayer Cu^{2+} spins, while the magnetic configuration for the kagome spins is rather hard to be determined due to their weak ordered moments.[29,30] The doping dependence of the ordered interlayer moment is shown in Fig. 1(d), which suggests that its value does not

change with doping. The decrease of the magnetic-peak intensities is mainly due to the substitution of nonmagnetic Zn^{2+} ions, which only occupy the positions of the interlayer Cu^{2+} as shown previously.[29] While our neutron-diffraction data cannot distinguish whether there is magnetic order for the $x = 0.3$ sample because of its very weak signal [Fig. 1(c)], previous μSR has shown that the magnetically ordered phase can survive up to 0.32.[32]

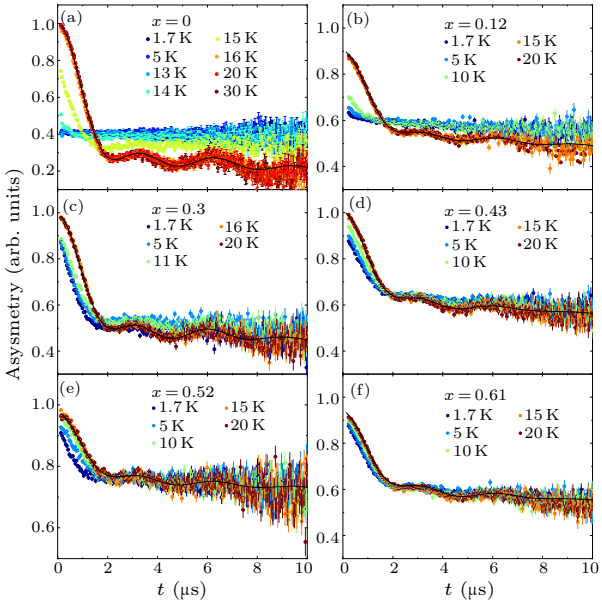

Fig. 2. (a)–(f) Time-dependent ZF μSR spectra at different temperatures for the $x = 0$, 0.12, 0.3, 0.43, 0.52 and 0.61 samples, respectively. The solid lines are fitted by Eq. (2).

Figure 2 provides the time-dependent ZF μSR spectra for the $Cu_{4-x}Zn_x(OH)_6FBr$ system. The data are normalized by the transverse field data at $H = 20$ Gauss and $T = 30$ K. At high temperatures, all of them show oscillations. With decreasing temperature, the oscillation is completely suppressed in the time range measured here for the low-doping samples but still presents for the middle doping samples. It has been shown that the oscillation is associated with both μ-OH and μ-F complexes.[32] The actual description of the μSR spectra in the AFM ordered state needs detailed information of the asymmetry at very low time scale close to zero, which is not accessible for our data. We thus simply introduce the following equation to account for the oscillation:

$$D_z^i(t) = \left[\frac{1}{3} + \frac{2}{3}\cos(\omega_i t)\right] e^{-\sigma_i^2 t^2}, \quad (1)$$

where i denotes the μ-OH and μ-F complexes for $i = 1$ and 2, respectively, and σ_i is associated with the distribution of nuclear fields surrounding the muon spin. Instead of using this simple function, one can employ a more accurate oscillation function, which depends on six frequencies.[32] However, since there are only about three periods in the raw data, we find that Eq. (1) is good enough and more stable in the fitting process. The time dependence of the asymmetry can be written as follows:

$$A(t) = A_0[fD_z^1(t) + (1-f)D_z^2(t)]e^{-\lambda t} + A_{\rm bg}, \quad (2)$$

where λ describes the weak electronic relaxation of the muons stopping in the sample and $A_{\rm bg}$ is a constant temperature-independent background for the muon stopping on the Ag sample holder. The factor f is introduced to account for different contributions from μ-OH and μ-F complexes. For all the samples measured here, f is obtained from the 30-K data and found to be 0.88. Compared to the analysis in Ref. [32], Eq. (2) can fit the μSR spectra for all the samples at all temperatures as shown in Fig. 2. This is important for us to understand the temperature dependence of the magnetic correlations. A similar function has also been used in studying the $Zn_xCu_{4-x}(OH)_6Cl_2$ system.[13]

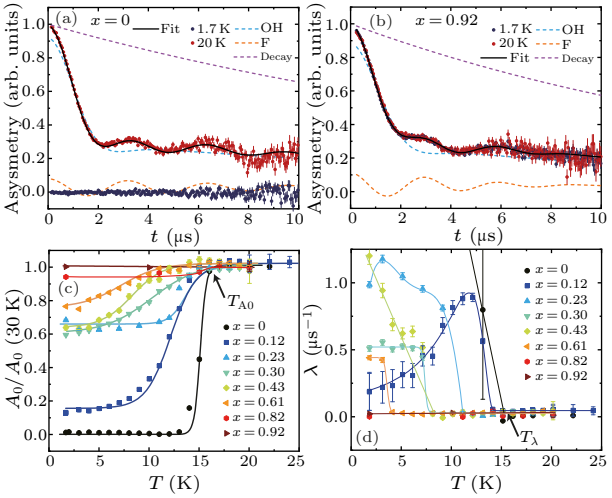

Fig. 3. [(a),(b)] Detailed analysis of the μSR spectra for the $x = 0$ and 0.92 samples, respectively. The solid lines show the results of the fit using Eq. (2). The blue and red dashed lines are contributions from the μ-OH and μ-F complexes, respectively. The purple dashed lines show the contribution from the exponential decay. [(c),(d)] Temperature dependence of $A_0/A_0(30\,K)$ and λ. The solid lines are guides to the eyes. The arrows in (c) and (d) mark the transition temperatures of A_0 and λ for the $x = 0$ sample, respectively.

Figures 3(a) and 3(b) further provide the detailed analysis of the muon spectra for the $x = 0$ and 0.92 samples, respectively. The initial fast drop of the asymmetry is mainly due to the μ-OH complex, while the μ-F complex mainly contributes to the oscillation above about 2 μs.[32] The relaxation term $\exp(-\lambda t)$ is also determined by the long-time data, which may be related to the μ-F complex. Figures 3(c) and 3(d) show the temperature dependence of the fitted parameters A_0 normalized by its 30-K value and λ, respectively. For the $x = 0$ sample, significant changes are found at T_N for both A_0 and λ. The temperatures are marked as T_{A_0} and T_λ, respectively. With increasing Zn substitution, both T_{A_0} and T_λ decrease but with

different rates. While the former is still above 10 K for the $x = 0.61$ sample, the latter has already dropped to about 4 K. For the $x = 0.82$ sample, we can still see a weak drop of A_0 but no change of λ can be seen down to the lowest temperature.

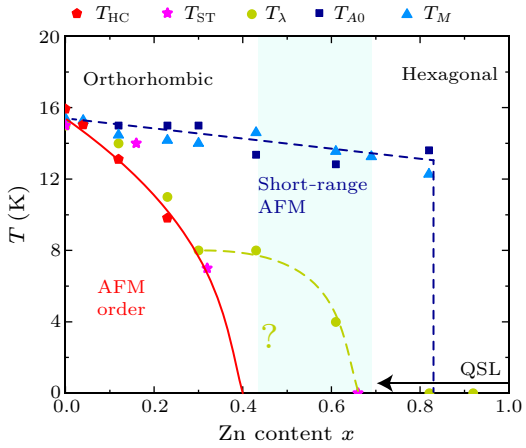

Fig. 4. Phase diagram of $Cu_{4-x}Zn_x(OH)_6FBr$. The AFM order is the long-range 3D magnetic order involving both the intralayer and interlayer spins. The nuclear structures for the low-doping and high-doping samples are orthorhombic and hexagonal, respectively, with the crossover happens in the doping range marked by the shaded area. The short-range AFM is from the interlayer Cu^{2+} ions. The question mark indicates the region between about 0.4 and 0.66 with an unknown ground state. The QSL ground state in the $x = 1$ sample may be extended down to 0.66, as shown by the arrow. T_{A_0} and T_λ are determined by the temperature dependence of A_0 and λ as shown in Figs. 3(c) and 3(d). T_{HC} and T_M are from the heat-capacity and magnetic-susceptibility measurements.[29] T_{ST} is from the temperature dependence of the frozen fraction from the μSR measurement reported previously.[32] The dashed lines are guides to the eyes.

Figure 4 gives the phase diagram of $Cu_{4-x}Zn_x(OH)_6FBr$ by summarizing our results and previous studies.[29,32] It has already been suggested[29] that the magnetic transition temperatures detected by the heat capacity and magnetic susceptibility, i.e., T_{HC} and T_M, is different in the Zn-substituted samples. Here we found that T_{HC} is close to T_{ST}, which is defined as the temperature where the frozen volume fraction obtained from the μSR spectra becomes nonzero.[32] Since both the heat capacity and frozen volume fraction are measuring the bulk properties, and our neutron-diffraction data also clearly show magnetic peaks up to $x = 0.23$, we conclude that the region for the long-range order AFM order are marked by T_{HC} and T_{ST}.

Figure 4 also demonstrates that T_M and T_{A_0} are very close to each other, suggesting that they have the same origin. As shown above, the value of A_0 is not the asymmetry at time zero but rather the extrapolated zero-time value after the very-fast initial drop that cannot be detected here. For the $x = 0$ sample, this kind of drop is due to the local fields from the long-range magnetic order.[32] With Zn substitution, the long-range order is suppressed but the magnetic clusters, most likely formed by the interlayer Cu^{2+} ions, can still survive and provide local magnetic fields to depolarize the muon spins, which will result in the fast initial drop of the asymmetry. This is consistent with previous discussions on the origin of the T_M.[29] Therefore, the area marked by T_M and T_{A_0} is associated with the short-range AFM from the interlayer moments. It should be noted that for low-doping samples, the system enters into the short-range AFM first and then becomes long-range magnetically ordered with decreasing temperature, which suggests that the long-range AFM order should involve kagome spins.

Tracing the doping dependence of T_λ shows that it follows the long-range AFM order initially but still persists up to $x = 0.61$ with the value of 4 K. T_λ is zero for the $x = 0.82$ sample, which suggests that it should become zero between $x = 0.61$ and 0.82. To nail down the exact doping level where T_λ becomes zero, we recall that the dynamical correlations obtained from the μsR measurements in the $x = 0.66$ and $x = 0.99$ samples are the same,[32] which indicates that they are in the same ground states. Therefore, T_λ should be zero at or below $x = 0.66$, as shown by the green-yellow dashed line. Therefore, the area between $x = 0.4$ and 0.66 below T_λ is the same area in Ref. [32] marked as the crossover regime between the static and dynamic ground states.

While it is still unclear what is the origin of this intermediate regime between the long-range AFM order and the QSL, there are a few results that may be related to it. First, the crossover from the orthorhombic to the hexagonal structure may also happen in the same doping range, as illustrated by the shaded area in Fig. 4. The change of the structure should result in the change of the exchange energies within the kagome planes. Second, the value of λ is mainly determined by the long-time relaxation and thus related to the μ-F complex. The position of the fluorine makes it not sensitive to interlayer spins, as shown by the ^{19}F NMR measurements.[23] As the low-energy spin excitations become gapped,[23,33] one expects that μSR spectra from the μ-F complex, which only detect very low-energy excitations, will not change with the temperature. These results suggest that the change of λ at low temperatures for $x < 0.66$ may be related to the kagome spins and the gapped QSL state in the $x = 1$ sample could be extended down to 0.66. It should be noted that the unknown crossover region labeled by the question mark and the QSL state should not be treated as within the short-range magnetic order, but rather as solely coming from the kagome spin system. In fact, our results suggest that above $x = 0.4$, the interlayer Cu^{2+} ions act as magnetic impurities that are separated from the kagome spin system and have

little effects on the latter.

In conclusions, we have established the magnetic phase diagram of the $Cu_{4-x}Zn_x(OH)_6FBr$ system via comparing several techniques.[29,32] The short-range spin correlations of the interlayer Cu^{2+} moments can persist up to $x \approx 0.82$, while the whole spin system only becomes long-range ordered below $x \approx 0.4$. The slow exponential decay of the long-time μSR spectra disappears above $x = 0.66$, which is consistent with a gapped QSL state. Our results suggest that the kagome and interlayer spin systems are decoupled at high-Zn-doping levels and may help us to further understand the actual magnetic ground state of the 2D kagome antiferromagnet $Cu_3Zn(OH)_6FBr$.

Y. W. and S. L. thank Dr. Chin-Wei Wang for his help.

References

[1] Messio L, Bernu B and Lhuillier C 2012 *Phys. Rev. Lett.* **108** 207204
[2] Bieri S, Messio L, Bernu B and Lhuillier C 2015 *Phys. Rev. B* **92** 060407
[3] Iqbal Y, Jeschke H O, Reuther J, Valentí R, Mazin I I, Greiter M and Thomale R 2015 *Phys. Rev. B* **92** 220404
[4] Gong S S, Zhu W, Yang K, Starykh O A, Sheng D N and Balents L 2016 *Phys. Rev. B* **94** 035154
[5] Liao H J, Xie Z Y, Chen J, Liu Z Y, Xie H D, Huang R Z, Normand B and Xiang T 2017 *Phys. Rev. Lett.* **118** 137202
[6] Mei J W, Chen J Y, He H and Wen X G 2017 *Phys. Rev. B* **95** 235107
[7] Wang Y C, Zhang X F, Pollmann F, Cheng M and Meng Z Y 2018 *Phys. Rev. Lett.* **121** 057202
[8] Savary L and Balents L 2017 *Rep. Prog. Phys.* **80** 016502
[9] Zhou Y, Kanoda K and Ng T K 2017 *Rev. Mod. Phys.* **89** 025003
[10] Norman M R 2016 *Rev. Mod. Phys.* **88** 041002
[11] Shores M P, Nytko E A, Bartlett B M and Nocera D G 2005 *J. Am. Chem. Soc.* **127** 13462
[12] Bert F, Nakamae S, Ladieu F, L'Hôte D, Bonville P, Duc F, Trombe J C and Mendels P 2007 *Phys. Rev. B* **76** 132411
[13] Mendels P, Bert F, de Vries M A, Olariu A, Harrison A, Duc F, Trombe J C, Lord J S, Amato A and Baines C 2007 *Phys. Rev. Lett.* **98** 077204
[14] Helton J S, Matan K, Shores M P, Nytko E A, Bartlett B M, Yoshida Y, Takano Y, Suslov A, Qiu Y, Chung J H, Nocera D G and Lee Y S 2007 *Phys. Rev. Lett.* **98** 107204
[15] de Vries M A, Stewart J R, Deen P P, Piatek J O, Nilsen G J, Rønnow H M and Harrison A 2009 *Phys. Rev. Lett.* **103** 237201
[16] Han T H, Helton J S, Chu S, Nocera D G, Rodriguez-Rivera J A, Broholm C and Lee Y S 2012 *Nature* **492** 406
[17] Han T H, Norman M R, Wen J J, Rodriguez-Rivera J A, Helton J S, Broholm C and Lee Y S 2016 *Phys. Rev. B* **94** 060409
[18] Fu M, Imai T, Han T H and Lee Y S 2015 *Science* **350** 655
[19] Khuntia P, Velazquez M, Barthélemy Q, Bert F, Kermarrec E, Legros A, Bernu B, Messio L, Zorko A and Mendels P 2020 *Nat. Phys.* **16** 469
[20] Nilsen G J, de Vries M A, Stewart J R, Harrison A and Rnnow H M 2013 *J. Phys.: Condens. Matter* **25** 106001
[21] Sun W, Huang Y X, Nokhrin S, Panb Y and Mi J X 2016 *J. Mater. Chem. C* **4** 8772
[22] Okuma R, Yajima T, Nishio-Hamane D, Okubo T and Hiroi Z 2017 *Phys. Rev. B* **95** 094427
[23] Feng Z, Li Z, Meng X, Yi W, Wei Y, Zhang J, Wang Y C, Jiang W, Liu Z, Li S, Liu F, Luo J, Li S, Zheng G Q, Meng Z Y, Mei J W and Shi Y 2017 *Chin. Phys. Lett.* **34** 077502
[24] Feng Z, Yi W, Zhu K, Wei Y, Miao S, Ma J, Luo J, Li S, Meng Z Y and Shi Y 2018 *Chin. Phys. Lett.* **36** 017502
[25] Puphal P, Zoch K M, Désor J, Bolte M and Krellner C 2018 *Phys. Rev. Mater.* **2** 063402
[26] Wei Y, Feng Z, dela Cruz C, Yi W, Meng Z Y, Mei J W, Shi Y and Li S 2019 *Phys. Rev. B* **100** 155129
[27] Iida K, Yoshida H K, Nakao A, Jeschke H O, Iqbal Y, Nakajima K, Ohira-Kawamura S, Munakata K, Inamura Y, Murai N, Ishikado M, Kumai R, Okada T, Oda M, Kakurai K and Matsuda M 2020 *Phys. Rev. B* **101** 220408
[28] Han T H, Singleton J and Schlueter J A 2014 *Phys. Rev. Lett.* **113** 227203
[29] Feng Z, Wei Y, Liu R, Yan D, Wang Y C, Luo J, Senyshyn A, dela Cruz C, Yi W, Mei J W, Meng Z Y, Shi Y and Li S 2018 *Phys. Rev. B* **98** 155127
[30] Tustain K, Nilsen G J, Ritter C, da Silva I and Clark L 2018 *Phys. Rev. Mater.* **2** 111405
[31] Smaha R W, He W, Jiang J M, Wen J, Jiang Y F, Sheckelton J P, Titus C J, Wang S G, Chen Y S, Teat S J, Aczel A A, Zhao Y, Xu G, Lynn J W, Jiang H C and Lee Y S 2020 *npj Quantum Mater.* **5** 23
[32] Tustain K, WardO-'Brien B, Bert F, Han T H, Luetkens H, Lancaster T, Huddart B M, Baker P J and Clark L 2020 arXiv:2005.12615 [cond-mat.str-el]
[33] Wei Y, Feng Z, Hu D H, Lohstroh W, dela Cruz C, Yi W, Ding Z F, Zhang J, Tan C, Shu L, Wang Y C, Wu H Q, Luo J, Mei J W, Meng Z Y, Shi Y and Li S 2017 arXiv:1710.02991
[34] Han T H, Isaacs E D, Schlueter J A and Singleton J 2016 *Phys. Rev. B* **93** 214416
[35] Zorko A, Nellutla S, van Tol J, Brunel L C, Bert F, Duc F, Trombe J C, de Vries M A, Harrison A and Mendels P 2008 *Phys. Rev. Lett.* **101** 026405
[36] Cépas O, Fong C M, Leung P W and Lhuillier C 2008 *Phys. Rev. B* **78** 140405
[37] Zorko A, Herak M, Gomilšek M, van Tol J, Velázquez M, Khuntia P, Bert F and Mendels P 2017 *Phys. Rev. Lett.* **118** 017202
[38] Laurita N J, Ron A, Han J W, Scheie A, Sheckelton J P, Smaha R W, He W, Wen J J, Lee J S, Lee Y S, Norman M R and Hsieh D 2019 arXiv:1910.13606 [cond-mat.str-el]
[39] Norman M R, Laurita N J and Hsieh D 2020 *Phys. Rev. Res.* **2** 013055
[40] Li Y, Pustogow A, Bories M, Puphal P, Krellner C, Dressel M and Valentí R 2020 *Phys. Rev. B* **101** 161115
[41] Rodriguez-Carvajal J 1993 *Physica B* **192** 55
[42] Arnold O, Bilheux J C, Borreguero J M, Buts A, Campbell S I, Chapon L, Doucet M, Draper N, Leal R F, Gigg M A, Lynch V E, Markvardsen A, Mikkelson D J, Mikkelson R L, Miller R, Palmen K, Parker P, Passos G, Perring T G, Peterson P F, Ren S, Reuter M A, Savici A T, Taylor J W, Taylor R J, Tolchenov R, Zhou W and Zikovsky J 2014 *Nucl. Instrum. Methods Phys. Res. Sect. A* **764** 156